Gluon radiation in top quark production and decay at e^+e^- colliders

Cosmin Macesanu* and Lynne H. Orr†
Department of Physics and Astronomy, University of Rochester, Rochester, New York 14627-0171
(Received 26 December 2000; published 29 November 2001)

We study gluon radiation in top quark production above threshold at high energy e^+e^- colliders. We allow for the top quarks to be off-shell, considering radiation in both the top production and decay processes simultaneously. Our calculation includes all top width effects, spin correlations, and b quark mass effects. We study the effects of gluon radiation on top mass reconstruction and examine the interference between production- and decay-stage radiation, which can be sensitive to the value of the top quark decay width.

DOI: 10.1103/PhysRevD.65.014004 PACS number(s): 14.70.Dj, 13.65.+i, 14.65.Ha

I. INTRODUCTION

By virtue of its large mass, the top quark is unique. Because it is so heavy, the top quark decays before it can form hadrons [1] and its spin information is passed along to its decay products. The top quark's mass is comparable to the electroweak symmetry breaking scale, and its Yukawa coupling is suspiciously close to unity. All of this means that top physics will be an important and interesting subject in the near future, and the top quark may lead us to physics beyond the standard model.

Future high energy lepton colliders—e^+e^- and $\mu^+\mu^-$—can provide relatively clean environments in which to study top quark physics. Although top production cross sections are likely to be lower at these machines than at hadron colliders, the color-singlet initial states give lepton machines some advantages. Furthermore, the fact that the laboratory and hard process center-of-mass frames coincide greatly simplifies the reconstruction of final states. In addition, many of the top quark's couplings, especially those to the photon and Z^0 boson, can be easily studied there.

The potential for precision studies of top physics at such colliders requires precision predictions from the theory, beyond leading order in perturbation theory. In particular, QCD corrections must be taken into account. Jets from radiated gluons can be indistinguishable from quark jets, complicating identification of top quark events from reconstruction of the top's decay products. To make matters worse, emission may occur in either the top production or decay processes, so that radiated gluons may or may not themselves be products of the decay. Subsequent mass measurements can be degraded, not only from misidentification of jets but also from subtle effects such as jet broadening when gluons are emitted near other partons.

In this paper we study the effects of real gluons radiated in top quark production and decay at e^+e^- colliders. We consider collision energies well above the top pair production threshold, so although for definiteness we will refer to electrons in the initial state, our parton-level results apply equally well to $\mu^+\mu^-$ collisions at the same energy. We allow for the top quarks to be off-shell, keeping the full width-dependent top propagator and retaining all spin correlations. Past treatments of QCD corrections have treated the top production [2] or decay [3] processes separately, or in one case [4] combined the two processes, but kept the on-shell (narrow-width) approximation. Gluon radiation for off-shell top has been treated previously in the soft gluon approximation [5,6]. Here we give an exact treatment for arbitrary gluon energies. We study properties of the emitted gluons, top mass reconstruction, and effects of interference between production- and decay-stage gluons that can be sensitive to the top quark width. Computation of the virtual QCD corrections for off-shell top is currently in progress [7] and will be combined with the present results for a full QCD next to leading order (NLO) treatment of top quark production and decay.

This paper is organized as follows. In Sec. II we discuss the matrix element calculation and Monte Carlo integration. We present numerical results in Sec. III, focusing on gluon distributions, mass reconstruction, and interference effects. We present our conclusions in Sec. IV. An Appendix includes some comments about gauge invariance.

II. CROSS SECTION CALCULATION

A. Computation of the matrix element

We compute the cross section for real gluon emission in top quark production and decay:

$$e^+e^- \to \gamma^*, Z^* \to t\bar{t}(g) \to bW^+\bar{b}W^-g. \tag{1}$$

At e^+e^- colliders, no gluons are radiated from the color-singlet initial state. Final-state gluon emission can occur in both the production and decay processes, with gluons emitted from the top or bottom quarks (or antiquarks), as shown in Fig. 1. Emission from the top quarks contributes to both production- and decay-stage radiation, depending on when the top quark goes on shell. Emission from the b quarks contributes to decay-stage radiation only. The separation of these contributions will be discussed below.

We compute the exact matrix elements for the diagrams shown in Fig. 1 with all spin correlations and the bottom mass included, using the helicity methods of Kleiss and Stirling [8]. Working at the matrix element, rather than the matrix element squared, level has the usual advantages of numerical efficiency, and in our case has the additional ad-

*Email address: mcos@pas.rochester.edu
†Email address: orr@pas.rochester.edu

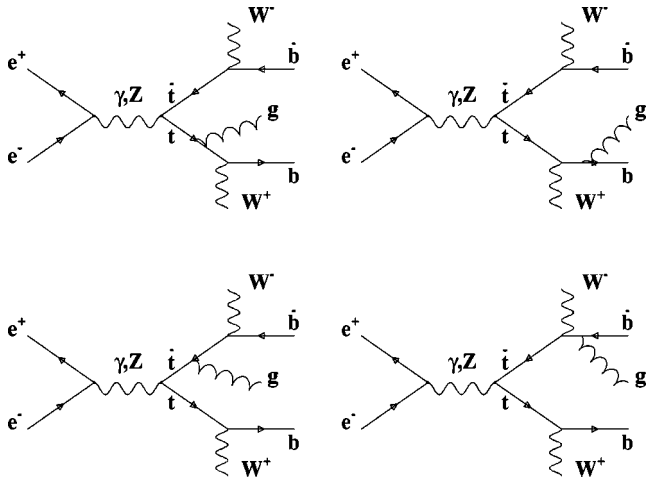

FIG. 1. Feynman diagrams for gluon emission in top production and decay at lepton colliders.

vantage that we can identify individual contributions and interferences between them. The explicit expressions for the matrix elements are complicated and not particularly illuminating, so we do not reproduce them here.[1]

We do not assume the top quark to be on shell; therefore we keep the finite top width Γ_t in the top quark propagator and include all interferences between diagrams. We use exact kinematics in all parts of the calculation. We do not include radiation from hadronic W decays; the W bosons are assumed to decay leptonically and we integrate over their decay products in the results presented here. In practice radiative hadronic W decays could be largely eliminated through invariant mass cuts, but a detailed study is required to determine exactly how effective this would be. We also note that because the W boson is a color singlet, radiative W decays cannot interfere (at first order) with the diagrams in Fig. 1. Any contributions from radiative W decays would therefore simply be additive even at the cross section level.

Some comments about gauge invariance are in order here. In the on-shell, or narrow-width, approximation, the top quarks are always on mass shell and the width is identically zero. In that case gauge invariance requires only diagrams with two intermediate top quarks. Once the top quarks are allowed to have a finite width and be off-shell, however, nonresonant diagrams—those with the same final state but only one or no intermediate top quarks—can also contribute. In the region of interest for top physics, viz., the region where the top quarks are nearly on shell, the poles in the doubly-resonant diagrams (those with two tops) cause their contributions to dominate. This is the motivation for the ''double-pole approximation'' in electroweak radiative corrections to W pair production [9]. In the present case we use invariant mass cuts (see below) to guarantee that we are in a region of the phase space where the doubly resonant diagrams—the only diagrams we include—dominate the cross section. We can restore gauge invariance using the approximation described in the Appendix. This gauge invariant result differs from the exact one by non-doubly-resonant terms, and this difference is very small numerically in the regions of interest.

B. Production-decay decomposition

As mentioned above, calculating at the amplitude level allows us to identify contributions from individual processes and their interferences. We are particularly interested in distinguishing between contributions from gluons radiated in the top quark production and decay stages. This is directly related to reconstruction of the top quark momentum from its decay products, which in an experiment allows us both to identify top events and to measure m_t. The presence of gluon radiation complicates the reconstruction because the emitted gluon may or may not be part of the top decay. If the gluon is not part of the decay, then it represents a correction to top production and should not be included in the top momentum reconstruction:

$$m_t^2 \approx p_t^2 = (p_b + p_W)^2 \equiv p_{bW}^2 . \tag{2}$$

If on the other hand the gluon is part of the decay, then it *should* be included in top reconstruction:

$$m_t^2 \approx p_t^2 = (p_b + p_W + p_g)^2 \equiv p_{bWg}^2 . \tag{3}$$

Being able to make this distinction turns out to be useful for purposes of efficient phase-space integration as well.

Although this production-decay distinction cannot be made absolutely in an experiment,[2] the various contributions can be separated in the calculation. For radiation from the b and $\bar{b}$ quarks, the assignment is easy: these contributions, corresponding to the two right-hand diagrams in Fig. 1, are clearly part of the top quark decay. However, as noted above, gluon emission from the top quark (or antiquark) contributes to both the production and decay stages; which stage depends on whether the top was closer to its mass shell before or after emitting the gluon. This condition corresponds to which of the two propagators from the top that emitted the gluon is numerically larger.

We can make the separation in our calculation as follows [6]. For definiteness, we consider gluon emission from the top quark, shown in the upper left diagram in Fig. 1. The matrix element for this diagram contains propagators for the top quark both before and after it radiates the gluon. The matrix element therefore contains the factors

$$\mathcal{M} \propto \left(\frac{1}{p_{Wbg}^2 - m_t^2 + i m_t \Gamma_t} \right) \left(\frac{1}{p_{Wb}^2 - m_t^2 + i m_t \Gamma_t} \right). \tag{4}$$

The right-hand side can be rearranged to give

[1] A FORTRAN program containing the matrix elements can be obtained from the authors.

[2] If the interference between processes is large this distinction is not even meaningful.

$$\mathcal{M} \propto \frac{1}{2p_{Wb}\cdot p_g}\left(\frac{1}{p_{Wb}^2 - m_t^2 + im_t\Gamma_t} - \frac{1}{p_{Wbg}^2 - m_t^2 + im_t\Gamma_t}\right). \tag{5}$$

This separates the production and decay contributions to the matrix element. The first term in parentheses contains a propagator that peaks when $p_{Wb}^2 = m_t^2$, which corresponds to the condition for production stage, as in Eq. (2). Similarly, the second term peaks for $p_{Wbg}^2 = m_t^2$, which corresponds to decay emission as in Eq. (3).

The complete amplitude can now be written schematically as

$$\mathcal{M}_{tot} = \mathcal{M}_{prod} + \mathcal{M}_{tdecay} + \mathcal{M}_{\bar{t}decay}. \tag{6}$$

The cross section, obtained from taking the absolute square of $\mathcal{M}_{tot}$, then contains separate production and decay contributions, from $|\mathcal{M}_{prod}|^2$ and $|\mathcal{M}_{tdecay}|^2, |\mathcal{M}_{\bar{t}decay}|^2$, respectively. It also contains cross terms representing the interferences, which in principle confound the separation but in practice are quite small.

The interference terms *are* interesting in their own right, although not for top reconstruction. In particular, the interference between production- and decay-stage radiation can be sensitive to the top quark width Γ_t [5,6], which is 1.42 GeV in the standard model at $\mathcal{O}(\alpha_s)$ [3]. The interference between for example the two propagators shown in Eq. (5) can be thought of as giving rise to two overlapping Breit-Wigner resonances. The peaks are separated roughly by the gluon energy, and each curve has width Γ_t. Therefore when the gluon energy becomes comparable to the top width, the two Breit-Wigners overlap and there can be substantial interference. In constrast, if the gluon energy is much larger than Γ_t, the overlap—and hence the interference—is negligible. Therefore the amount of interference serves as a measure of the top width. We will explore this more below.

The integration over the final state phase space to obtain the cross section involves an integrand that contains multiple Breit-Wigner peaks from the top quark propagators as well as infrared singularities when the gluon energy becomes small. Even with cuts on E_g, the rapid variation of the integrand can spoil the integration procedure. To eliminate this problem, we tailor the momentum generator to the production of a gluon in association with two massive particles ($\gamma^*, Z^* \to t\bar{t}g$ or $t \to bWg$). The multiple Breit-Wigner peaks are taken into account by using a multi-channel approach that integrates separately over the individual production and decay contributions; the Breit-Wigner behavior is smoothed out in the phase space generation. The interference terms, which have products of Breit-Wigners that peak in different places, much like in Eq. (4), are integrated using a combination of the three main channels.

III. NUMERICAL RESULTS

In this section we show results of the numerical calculation described above. We present the cross section for $b\bar{b}W^+W^-g$ production in e^+e^- collisions at a 500 GeV center-of-mass energy, with a few exceptions which are clearly identified. The calculation is entirely at the parton level, and we do not include initial state radiation, beam energy spread, or beamstrahlung.[3] We use the following numerical values of parameters: $m_t = 175$ GeV, $m_b = 5$ GeV, $M_W = 80$ GeV, $\Gamma_t = 1.42$ GeV, and $\alpha_s = 0.1$. Note that α_s appears simply as an overall factor, because all of our events contain a gluon.

Unless otherwise indicated, we use the following cuts. We require $E_g > 5$ GeV to eliminate the infrared singularity and because we intend for the gluon to be detectable. In addition we wish the gluon to be separable from the b and $\bar{b}$ quark; this is implemented via the requirement $m_{bg}, m_{\bar{b}g} > 10$ GeV, which we shall identify below as "m_{bg} cuts." (Separation could also be achieved with a cut on the gluon's E_T with respect to the b or $\bar{b}$; the choice makes little difference in the resulting distributions.) In order to make sure that we do not get contributions to our results from regions of the phase space where non-doubly-resonant diagrams might be important, we require

$$160 \text{ GeV} \leqslant m_{bW} \leqslant 190 \text{ GeV}$$

or

$$160 \text{ GeV} \leqslant m_{bWg} \leqslant 190 \text{ GeV} \tag{7}$$

and the same thing for the $\bar{b}$. These conditions will be identified as "m_t cuts" below.

A. Characteristics of the gluon radiation

We begin with the relative contributions of production- and decay-stage radiation to the total cross section. Figure 2 shows the fraction $\sigma_{prod}/\sigma_{tot}$ of the total cross section due to production stage emission in events with an extra gluon, as a function of the minimum energy of the gluon. The cross section σ_{prod} is computed by integrating $|\mathcal{M}_{prod}|^2$ only [cf. Eq. (6)] over the allowed phase space; σ_{tot} is computed using $|\mathcal{M}_{tot}|^2$. The figure contains no cuts besides that on gluon energy and is simply meant to illustrate how radiation is apportioned in top production and decay for different center-of-mass energies; the solid line corresponds to c.m. energy 1 TeV, and the dashed line is for 500 GeV. Both curves fall off as the minimum gluon energy increases; this reflects the decrease in phase space for gluons radiated in the production stage. We see that the production fraction is always higher at 1 TeV collision energy than at 500 GeV. This too reflects phase space — for a given gluon energy there is more phase space available to produce gluons in association with top pairs at the higher c.m. energy. However both fractions remain below 0.5; decay-stage radiation always dominates at these energies.

Figure 3 shows for a 500 GeV center-of-mass energy the effect on the production fraction of separation cuts between

[3]These effects can reduce the collision energy and total cross section. The shapes of our distributions are not sensitive to the total energy, but we expect their normalization to be somewhat reduced when these effects are included.

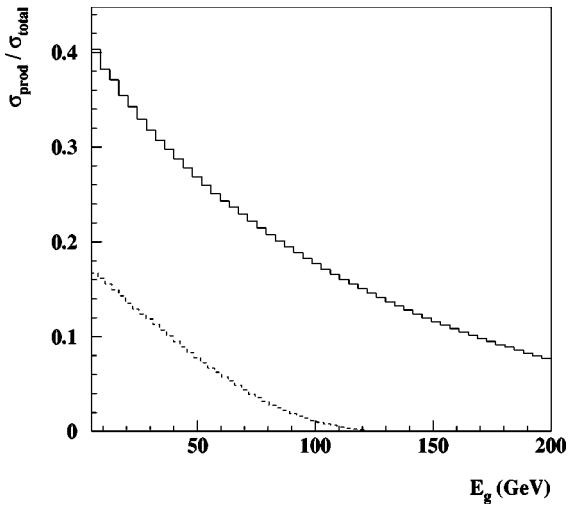

FIG. 2. The fraction of gluon emissions radiated in the production stage, as a function of minimum gluon energy, for center-of-mass energy 1 TeV (solid line) and 500 GeV (dashed line), with no cuts.

the gluon and b quarks. The dashed line shows the fraction with no cuts. The dotted line corresponds to requiring that the transverse energy of the gluon with respect to the b and $\bar{b}$—which we denote $E_T(g,b)$—be greater than 3 GeV. The solid line corresponds to the cut $m_{bg}>10$ GeV where the b can either be a quark or antiquark. The effect of both of these cuts is to eliminate gluons that are soft and/or close to one of the bottom quarks; since these contributions tend to come from decay-stage radiation, their effect is to increase the fraction of production-stage radiation. If the b were massless there would be a collinear singularity in the decay contribution; this does not happen in our case but the decay distribution still peaks when the b-quark–gluon angle is small. The effects of both cuts become smaller with increasing gluon energy.

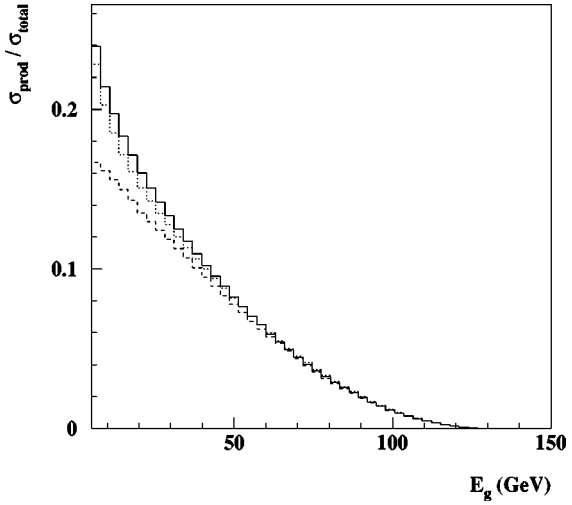

FIG. 3. The fraction of gluon emissions radiated in the production stage, as a function of minimum gluon energy, for center-of-mass energy 500 GeV, with no cuts (dashed line), $E_T(g,b)>3$ GeV (dotted line), and $m_{bg}>10$ GeV (solid line).

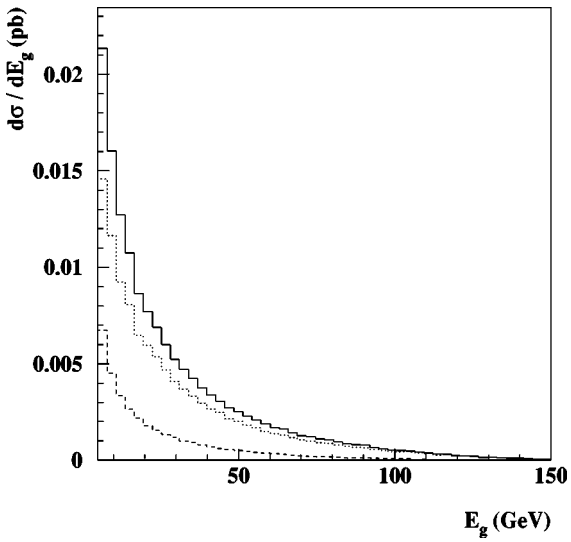

FIG. 4. The spectrum of radiated gluons as a function of gluon energy in GeV for center-of-mass energy 500 GeV, with m_{bg} and m_t cuts (see text). Dashed histogram: production-stage radiation. Dotted histogram: decay-stage radiation. Solid histogram: total.

Figure 4 shows the total gluon energy spectrum for a collision energy of 500 GeV along with its decomposition into production (dashed histogram) and decay (dotted histogram) contributions. The interferences between the two are negligible and are not shown; this will be true for all subsequent figures until we consider the interference explicitly. Included in this figure are the m_t and m_{bg} cuts discussed above. As indicated in the previous figures, radiation from the top decays dominates. Otherwise the spectra are not vastly different; both exhibit the rise at low energies due to the infrared singularity characteristic of gluon emission, and both fall off at high energies as phase space runs out.

B. Mass reconstruction

We now turn to the question of mass reconstruction in the presence of a radiated gluon. For events that contain a hard gluon, we wish to consider invariant mass distributions reconstructed according to different scenarios. In particular, we wish to determine how best to assign the gluon (to top production or decay) in such events. Figure 5 shows top invariant mass distributions with and without the extra gluon included; the first plot shows the distribution in m_{bW} and the second shows[4] m_{bWg}. We have imposed m_{bg} cuts and required $E_g>5$ GeV. In both cases there is a clear peak at the correct value of m_t. Note that the peak in the first plot contains the production contribution as expected, but the radiative decay part contributes as well. This is because even for decay-stage radiation, only one of the produced t quarks de-

[4]We do not address the details of reconstruction of final state parton momenta from experimentally observed quantities, and we assume that mass constraints along with energy and momentum conservation allow this reconstruction even in the case of leptonic W decay. These issues should be examined more closely in a more thorough analysis.

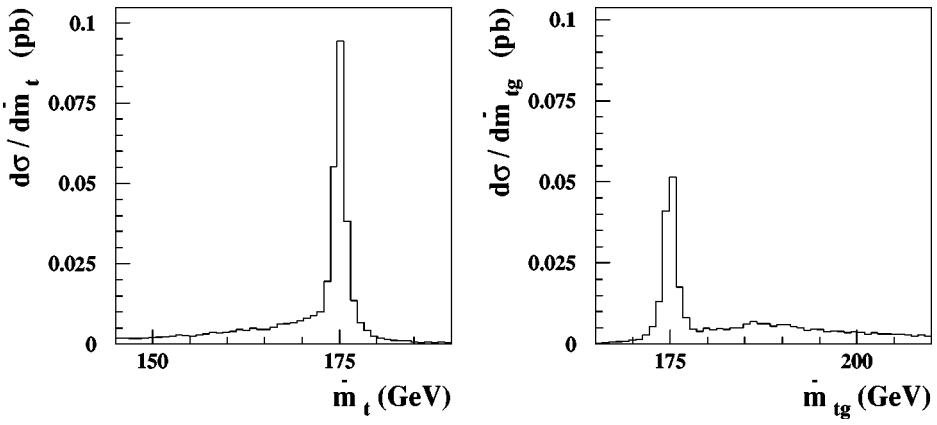

FIG. 5. The top invariant mass spectrum without (left) and with (right) the gluon momentum included, for center-of-mass energy 500 GeV, with m_{bg} cuts and $E_g > 5$ GeV.

cays radiatively; the other still has $p_t^2 = p_{bW}^2$ and therefore contributes to the m_{bW} peak. The long tails in the two distributions are from misassignments of the gluons. In the left-hand plot, where the gluon is not included in the reconstruction, we see a low-side tail due to events where the gluon was radiated in the decay but was not included in the reconstruction. Similarly, in the right-hand plot we see a high-side tail due to events where the gluon was radiated in association with production, and was included when it should not have been.

We wish to define a single distribution for the top mass that combines both types of events yet omits wrong combinations as much as possible. One possibility is to cut on the angle between the gluon and the b quark, whose distribution we show in Fig. 6. This is motivated by the fact that gluons radiated from the b quarks are always part of the decay, and such gluons tend to be emitted close to the b quark direction. As we have mentioned, the mass of the b quark prevents a collinear singularity, but the gluon distribution still peaks close to the b, as can be seen in the figure. In order to verify the correlation between the $b-g$ angle and the stage at which the gluon is radiated, we decompose the distribution

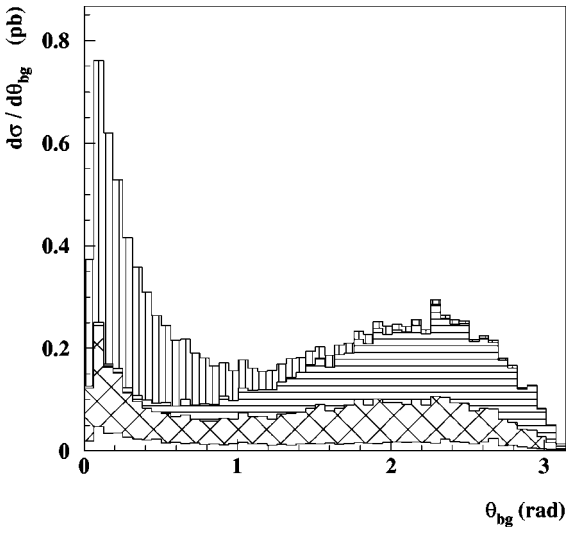

FIG. 6. The distribution in the angle between the gluon and the b quark for center-of-mass energy 500 GeV, with $E_g > 5$ GeV. The various contributions are as described in the text.

in θ_{bg} into various invariant mass regions. (Here we refer to the b quark only, and not the $\bar{b}$.) Using the variables $\tilde{m}_t = m_{bW^+}$, $\tilde{m}_{tg} = m_{bW^+g}$, $\tilde{m}_{\bar{t}} = m_{\bar{b}W^-}$, and $\tilde{m}_{\bar{t}g} = m_{\bar{b}W^-g}$ we define four types of events:

type 1: 172 GeV$< \tilde{m}_{tg}$, $\tilde{m}_{\bar{t}} <$178 GeV (vertical hatching)
type 2: 172 GeV$< \tilde{m}_t$, $\tilde{m}_{\bar{t}g} <$178 GeV (horizontal hatching)
type 3: 172 GeV$< \tilde{m}_t$, $\tilde{m}_{\bar{t}} <$178 GeV (cross hatching)
type 4: any other event (no hatching).

Type 1 events are dominated by contributions from radiative t decays, and we can see that they do tend towards the b quark direction. Type 2 events (horizontal hatching) are in turn dominated by radiative $\bar{t}$ decays; gluons in this case tend to cluster near the $\bar{b}$ direction, and since the b and $\bar{b}$ tend to appear in opposite hemispheres, type 2 gluons are mostly found at large angles to the b. Events of type 3 (cross hatching) are mostly production-stage contributions; their distribution is more or less uniform, independent of the b quark direction. Finally, events of type 4 (no hatching) get contributions from both production and decay, with no compelling evidence for one over the other.

Using this figure we can make the following conventions:

if $\theta_{bg} < 0.7$ rad, assign gluon to t decay
if $\theta_{\bar{b}g} < 0.7$ rad, assign gluon to $\bar{t}$ decay
if $\theta_{bg}, \theta_{\bar{b}g} > 1$ rad, assign gluon to $t\bar{t}$ production.

With these cuts on the proximity of the gluon to the b quark, we construct the top mass distribution presented in the dotted histogram in Fig. 7.

Of course an important reason the cuts are so effective is that we work at the parton level. The experimentalists do not have that luxury, and, as one would expect, hadronization and detector effects are likely to cloud the picture. The solid histogram in Fig. 7 shows the mass distribution after including energy smearing; the solid curve is a Breit-Wigner fit. The spread in the measured momenta of the final state particles is parametrized by Gaussians with widths $\sigma = 0.4\sqrt{E}$ for quarks and gluon, and $\sigma = 0.15\sqrt{E}$ for the W's. We see that the central value does not shift, but the distribution becomes significantly wider.

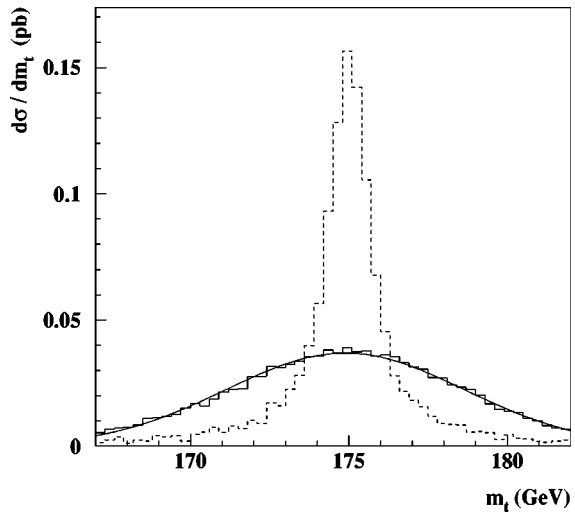

FIG. 7. The top invariant mass spectrum with b-gluon angle selection criteria (dotted histogram), for center-of-mass energy 500 GeV, minimum gluon energy 5 GeV, and m_{bg} cuts. The solid curve and histogram show the effects of energy smearing.

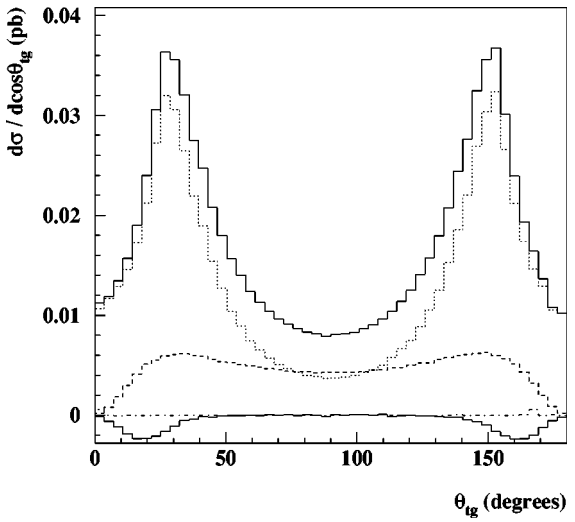

FIG. 8. The distribution in angle between the top quark and the gluon for gluon energies from 5 to 10 GeV, $\cos\theta_{tb}$,$\cos\theta_{\bar{t}b}<0.9$, m_t cuts, and 750 GeV collision energy. The upper solid histogram is the total and the other histograms represent the individual contributions: dotted: decay; dashed: production; dot-dashed: decay-decay interference; solid: production-decay interference.

These results are meant to give an indication of the effects of hard gluon radiation on mass reconstruction and how they might be dealt with. Other variables to consider in choosing the cuts are m_{bg}, the transverse energy of the gluon with respect to the b or $\bar{b}$, or some combination of energies and angles as defined in the various algorithms used in jet definitions for e^+e^- colliders. At tree level and with partons only, the exact choice is not very important.

The measurement of the top mass from momentum reconstruction will be dominated by contributions from the Born amplitude. A complete analysis also requires inclusion of the real corrections discussed here as well as the virtual corrections computed in [7]. In addition, initial state radiation, beam energy spread, and beamstrahlung must be taken into account along with hadronization and detector effects. It has been estimated in [11] that a statistical precision of 200 MeV may be achievable in the dilepton mode, but a complete analysis has not yet been performed.

It should be noted that the mass which is measured from momentum reconstruction at a collider is the pole mass. This is to be distinguished from threshold masses ($1S$, low-scale, PS, $\overline{PS}$) which are measured from the shape of the total cross section at the top pair production threshold; threshold mass measurements to better than 100 MeV are anticipated (see [12] and references therein). There is an $\mathcal{O}(\Lambda_{QCD})$ renormalon ambiguity associated with the pole mass which does not plague the threshold masses; therefore the relation between the pole and threshold masses also contains the renormalon ambiguity. See [13] for further discussion.

C. Interference and sensitivity to Γ_t

Finally, we return to the subject of interference. As mentioned above, the interference between the production- and decay-stage radiation can be substantial for gluon energies close to the total width of the top quark Γ_t; the interference is therefore sensitive to the value of Γ_t. However, because this interference is in general small, we need to find regions of phase space where it is enhanced. This question was considered in [6] in the soft gluon approximation,[5] where it was found that the interference was enhanced when there was a large angular separation between the t quarks and their daughter b's.

Here we examine whether the result of [6], which considered a fixed final-state configuration, survives the exact calculation and phase space integration. Figure 8 shows that it does. There we plot the distribution in the angle between the emitted gluon and the top quark for gluon energies between 5 and 10 GeV and with $\cos\theta_{tb}<0.9$ and m_t cuts. The center-of-mass energy is 750 GeV. This c.m. energy is chosen because for there to be significant interference between production and decay-stage radiation, both contributions must be sizable. At 500 GeV, we see from Figs. 2 and 3 that the production contribution is suppressed compared to that from decay; as a result, the interference is very small. Increasing the energy increases the production-stage contribution. We note that the distributions at 750 GeV and 1 TeV do not differ substantially.

The histograms in Fig. 8 show the decomposition into the various contributions. The production-stage radiation is shown as a dashed histogram; we see that it reaches its largest values at relatively small and large angles. Small angles correspond to the t direction, and large angles more or less to the $\bar{t}$ direction, since for the small gluon energies of interest here, the t and $\bar{t}$ are nearly back-to-back. The dotted histogram represents the decay-stage contribution; it dominates the cross section and peaks in the same region as the production contribution. This leads to substantial production-decay

[5]See also [5,10].

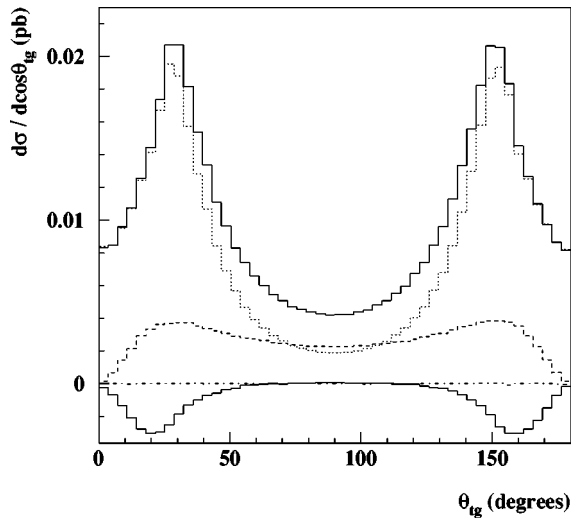

FIG. 9. As in Fig. 8, with the addition of the cuts given in Eqs. (9),(10).

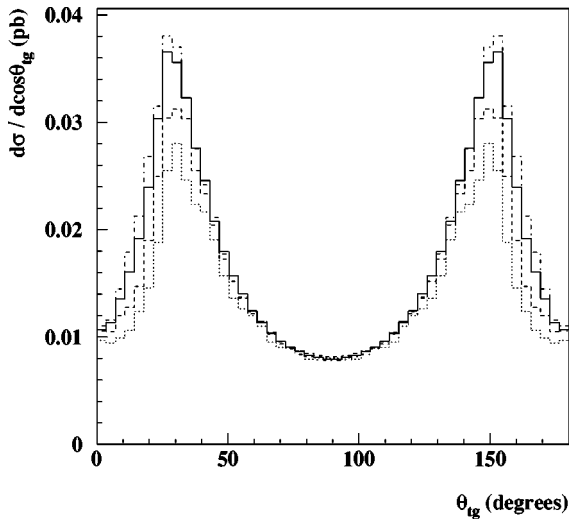

FIG. 10. The distribution in angle between the top quark and the gluon for gluon energies from 5 to 10 GeV, cos θ_{tb},cos $\theta_{\bar{t}b}<0.9$, and 750 GeV collision energy. The histograms correspond to different values of the top width Γ_t: dot-dashed: 0.1 GeV; solid: 1.42 GeV (SM); dashed: 5. GeV; dotted: 20 GeV.

interference, shown as the negative solid histogram. This interference is destructive, so that it serves to *suppress* the total cross section, shown as the positive solid histogram. This effect would be enhanced if we lowered the gluon energies to values closer to Γ_t, but jets from very low energy gluons are not likely to be observable, so we cut off the gluon energy at 5 GeV. Finally, interference between the emissions in the t and $\bar{t}$ decays is shown as a dot-dashed histogram, but as there is very little overlap between the two phase space regions even with these cuts, this contribution is negligible.

The cuts we have used are fairly generic; we can further enhance the interference terms with a judicious choice of additional cuts. If we examine their behavior in more detail in various regions of phase space, we find that the sign of the interference terms depends on the value of invariant mass of the top quark. Since we integrate over this mass, we get cancellations (a similar effect ensures cancellations of nonfactorizable corrections in inclusive quantities).

Consider the interference between radiation in the production stage and the top decay stage. The product of the two Breit-Wigner peaks is proportional to the factor

$$f_t=(p_{Wb}^2-m_t^2)(p_{Wbg}^2-m_t^2)+m_t^2\Gamma_t^2. \tag{8}$$

This factor will multiply a quantity which, upon integration over angles, is negative. Therefore, for invariant mass values such that f_t is positive, the interference terms are negative, while for negative f_t, the interference terms are positive. We can impose cuts that take advantage of this: if we require the invariant masses to satisfy

$$f_t>0, \quad \text{if} \quad \theta_{bg}<\theta_{\bar{b}g}; \tag{9}$$

$$f_{\bar{t}}>0, \quad \text{if} \quad \theta_{bg}>\theta_{\bar{b}g}, \tag{10}$$

we obtain the distribution shown in Fig. 9. The interference effects are enhanced, though at the cost of a substantial decrease in cross section.

Because the production-decay interference is destructive, increasing the top width would further suppress the total distribution. The height of the peaks, then, is sensitive to the value of Γ_t. This is illustrated in Fig. 10, which shows the cross section [without the cuts of Eqs. (9),(10)] for different values of the top width,[6] ranging from 0.1 GeV to 20 GeV. The SM case ($\Gamma_t=1.42$ GeV) is shown as a solid line. It is interesting to note that in the context of perturbative gluon radiation, the SM top width is actually a small quantity. There are several other points to note. In principle, this sensitivity to Γ_t gives us a method to measure the top quark's total width, independent of decay mode, above the top production threshold. Although in practice statistics would surely limit the possible precision of such a measurement, the total top width is not so easy to measure directly by any means. Furthermore, the effects illustrated here arise from simple quantum-mechanical interference, and finding experimental evidence for interference between the radiation at the various stages is an interesting goal by itself.

IV. CONCLUSION

In summary, we have presented results from an exact parton-level calculation of hard gluon radiation in off-shell top production and decay above threshold at lepton colliders, with the b quark mass and finite top width, as well as all spin correlations and interferences included. We have decomposed the cross section into the separate contributions from emissions associated with top production, t and $\bar{t}$ decay, and

[6]The histograms here are scaled so that they all would have the same normalization in the absence of interference effects. Without this rescaling, changing the width while keeping the tbW coupling fixed changes the total cross section, which behaves like $1/\Gamma_t^2$ for small Γ_t.

their interferences. We have indicated some of the issues associated with this gluon radiation in top mass reconstruction and top width sensitivity in the gluon distribution. A detailed treatment of many of these issues, in particular with regard to mass reconstruction, will be presented in forthcoming work which combines virtual and real QCD corrections to this process into a complete NLO computation of top production and decay.

ACKNOWLEDGMENTS

We thank C. R. Schmidt and W. J. Stirling for helpful correspondence and discussions. This work was supported in part by the U.S. Department of Energy, under grant DE-FG02-91ER40685 and by the U.S. National Science Foundation, under grant PHY-9600155.

APPENDIX: GAUGE INVARIANCE

Our results include only diagrams with two intermediate top quarks. Because these top quarks are not assumed to be on shell, our result is not strictly gauge invariant. We can obtain a gauge invariant answer by subtracting some non-doubly resonant terms as follows. Consider the diagram where the gluon is radiated by the top quark (the first diagram in Fig. 1). The contribution of this diagram to the production amplitude is (with $\hat{a} \equiv a^\mu \gamma_\mu$ and $k \equiv p_g$):

$$\mathcal{M}^{(t)}_{prod} \sim \frac{1}{2k\cdot p_{Wb}} \overline{u}(b)\hat{\epsilon}_W \frac{\hat{p}_{Wb}+m_t}{p^2_{Wb}-\overline{m_t^2}} \times \hat{\epsilon}_g(\hat{p}_{Wb}+\hat{k}+m_t)\ldots v(\overline{b}). \quad \text{(A1)}$$

By commuting $\hat{\epsilon}_g$ to the right, this can be written

$$\mathcal{M}^{(t)}_{prod} \sim \frac{1}{2k\cdot p_{Wb}} \overline{u}(b)\hat{\epsilon}_W \times \frac{(\hat{p}_{Wb}+m_t)(2\epsilon_g\cdot p_{Wb}+\hat{\epsilon}_g\hat{k})-(p^2_{Wb}-m_t^2)\hat{\epsilon}_g}{p^2_{Wb}-\overline{m_t^2}}\ldots \times v(\overline{b}). \quad \text{(A2)}$$

The term which breaks gauge invariance here is the one proportional to $(p^2_{Wb}-m_t^2)$. This is a non-resonant term, regardless of the gluon being radiated in production or decay stage (in other words, regardless of $p^2_{Wb}\approx m_t^2$ or $p^2_{Wbg}\approx m_t^2$); therefore, in keeping with the approximation used, we can neglect it.

A similar analysis works for the contribution of this diagram to the top decay amplitude, with p_{Wb} replaced by p_{Wbg} in this case, and we drop a term proportional to $(p^2_{Wbg}-m_t^2)$. Finally, the amplitudes corresponding to the diagram in which the gluon originates from the $\overline{t}$ can be computed in the same manner. The final result is gauge invariant, and differs from the exact result by non-doubly-resonant terms, as we have shown.

We have implemented the above computation in the Monte Carlo program, and have generated all the distributions presented in the paper using the gauge invariant amplitude. Numerically, the difference between the gauge invariant result and the exact result is very small (of order 0.01% of the total cross section, and order 1% with respect to the interference terms). This indicates that the other non-doubly resonant contributions (coming from diagrams with a single top or none) are also small; a more detailed study is in progress.

Finally, we note that this method for restoring gauge invariance is not unique. We could, for example, have instead replaced the top mass in the top propagator numerator with the invariant masses: $\sqrt{p^2_{Wb}}$ in the production amplitude, and $\sqrt{p^2_{Wbg}}$ in the decay amplitudes. The result is also gauge invariant, and also differs from the exact result by non-resonant terms.

[1] I. I. Bigi *et al.*, Phys. Lett. B **181**, 157 (1986); L. H. Orr and J. L. Rosner, *ibid.* **246**, 221 (1990); **248**, 474(E) (1990); L. H. Orr, Phys. Rev. D **44**, 88 (1991).

[2] J. Jersak, E. Laerman, and P. Zerwas, Phys. Rev. D **25**, 1218 (1982); Yu. L. Dokshitzer, V. A. Khoze, and W. J. Stirling, Nucl. Phys. **B428**, 3 (1994).

[3] M. Jezabek and J. H. Kuhn, Nucl. Phys. **B314**, 1 (1989); A. Czarnecki, Phys. Lett. B **252**, 467 (1990); C. S. Li, R. J. Oakes, and T. C. Yuan, Phys. Rev. D **43**, 3759 (1991).

[4] C. R. Schmidt, Phys. Rev. D **54**, 3250 (1996).

[5] G. Jikia, Phys. Lett. B **257**, 196 (1991).

[6] V. A. Khoze, L. H. Orr, and W. J. Stirling, Nucl. Phys. **B378**, 413 (1992).

[7] C. Macesanu, in *Fermilab 2000: Physics and Experiments With Future Linear e^+e^- Colliders*, edited by A. Para and H. E. Fisk (AIP, Melville, NY, 2001), p. 352; and (in preparation).

[8] R. Kleiss and W. J. Stirling, Nucl. Phys. **B262**, 235 (1985).

[9] A. Denner, S. Dittmaier, M. Roth, and D. Wackeroth, Nucl. Phys. **B587**, 67 (2000).

[10] G. Siopsis, Phys. Rev. D **58**, 014009 (1998).

[11] J. Antoš and G. P. Yeh, *Sitges 1999: Physics and Experiments With Future Linear e^+e^- Colliders*, edited by E. Fernández and A. Pacheco (Universitat de Barcelona, Barcelona, 1999), p. 234.

[12] American Linear Collider Working Group Collaboration, T. Abe *et al.*, "Linear collider physics resource book for Snowmass 2001," SLAC-570, hep-ex/0106055; hep-ex/0106056; hep-ex/0106057; hep-ex/0106058.

[13] A. H. Hoang *et al.*, EPJdirect **3**, 1 (2000).